C12 -Modern approaches for real time state estimation

12.1. Overview

Bus voltages in electric networks are complex values, defined by a magnitude and a phase (angle) computed using a reference value. Mathematically, the voltage can be represented as a sinusoidal or a phasor quantity, as in Fig. 12.1

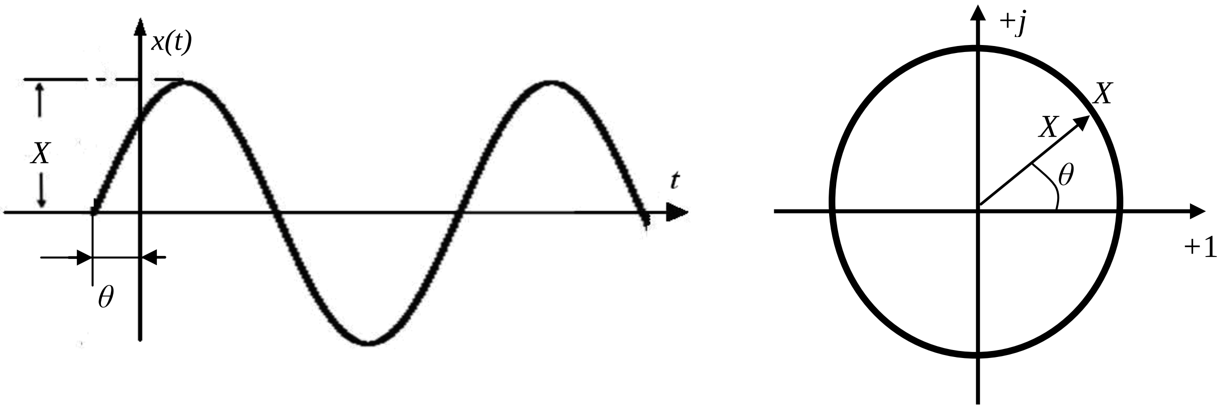

$$x(t) = X \cdot \sin(\omega t + \theta) \qquad \vec{X} = X \cdot e^{j\cdot\theta}$$

Fig. 12.1- A physical quantity represented as sine wave and a phasor

The phase difference of the voltage is the difference between the angles of two voltages, when the same reference is used. In an AC system, the active powers flow from buses with higher bus voltage angle values to buses with lower voltage angle value, and the amount of transferred power is larger when the phase difference is larger. Because of this, knowing the exact values of bus voltage angles in the system can give a real time snapshot of the system, usable in decision making and optimal operation of the system. But a key requirement for achieving this is having accurate and synchronized angle measurements from the system.

12.2. Phasor measurement units (PMU)

Traditional SCADA/EMS systems provide a measurement sampling rate of seconds. For angle measurements, this translates into heavy synchronization errors. Until recently, this problem made impossible the use of voltage angle measurements in real time state estimation analysis.

With the development of the Global Positioning System (GPS) and modern communication infrastructures, high technology digital metering devices became able to provide high precision time synchronized measurement, capable of sampling rates to up to microseconds and numeric conversion to phasors. This type of device is known as phasor measurement unit (PMU), and the technology behind it is called synchronized phasor measurement (SPM).

Phasors can be computed from measured values in several ways. The simplest of them uses an unique base frequency which is used to compute the magnitude and angle phasors thorought the EPS. In real conditions, however, the frequency is variable, even if in a very narrow range, which leads to a different angle value.

More precise phasor estimation methods use Kalman filters [Bukh 2007] or artificial neural networks. [Jordan 2008]. One of the most used methods is based on the Fourier transform, which determines the $\vec{X}$ phasor as:

$$\vec{X} = X_R + j \cdot X_I = \frac{\sqrt{2}}{N} \sum_{k=1}^{N} x_k \cdot e^{-j \cdot \frac{2 \cdot \pi \cdot k}{N}} = \frac{\sqrt{2}}{N} \sum_{k=1}^{N} x_k \cdot \left(\cos \frac{2 \cdot \pi \cdot k}{N} - j \cdot \sin \frac{2 \cdot \pi \cdot k}{N} \right) \tag{12.1}$$

where N is the number of samples used to represent a period of the measured signal and x_k are the measured signals.

Uses of PMUs in industry

In the power systems field, PMUs are installed in key buses from the system, from where they continuously transmit phasor values for bus voltages and currents on the branches connected to the respective buses. If the PMUs are interconnected through a communication system, they are functioning as a control and real time monitoring system. The configuration of such a system depends largely on its purposes and of the available investment resources.

Mainly, three types of such networks exist [Karlsson 2004]:

- The simplest way of employing PMUs in the existing control and monitoring system is to use the already existing EMS/SCADA infrastructure, but this is a limited capabilities solution and it is recommended to be used just as a starting point.
- Flat network architectures, which use as terminals intelligent protection devices able for network acquired or local data processing; this variant is feasible for distance protection or voltage and frequency stability systems.
- Multilayer network architectures, where PMUs are connected to data concentrators which can act as simple collectors or as processing units. Further, the local data concentrators are connected to a central data processor located inside the dispatcher's center of operation. This variant can be used at local and central level, for system monitoring, state estimation etc. A diagram of such a network is shown in Fig. 12.2.

The development of PMU technology started back in the 70's. The chronological landmarks can be summarized as follows:

- late 1970s – the first NAVSTAR satellite is launched. Later, the project would change its name to Global Positioning System (GPS)
- 1981 – Bonanomi proposes a global time synchronization method that uses radio signals, suggesting the NAVSTAR system as synchronization tool [Bonanomi 1981]
- mid 1980s – the first attempts to use the GPS system in SPM technology
- 1983 – Professor Phadke from Virginia Polytechnic Institute proposes a new method for measuring and computing phasors, which uses a direct sequence voltmeter equipped with digital filters [Phadke et al 1983]
- 1988 – Professor Phadke develops the first PMU
- 1991 – The Macrodyne Company produces the first commercial PMU [Phadke 2002], [Martin 2008].

Fig. 12.3 presents two PMU devices built by Macrodyne (a) and General Electric (b) [webMicro1, webGE1]

12.3. SPM application in power systems

The SPM-PMU technology found numerous applications in power systems analysis. Some of these applications are described in brief [Gavrilaş 09].

Real-time monitoring and control of power systems

Knowledge of real-time information is a critical tool for the system operator. The dispatcher can have a clear image of the actual state of the system, to see or anticipate unwanted events that may occur. The static and dynamic state visualization of the system are some of the most important applications of the SPM technology. Figure 12.4 is an example of voltage level monitoring during the events that preceded and followed the wide area blackout that took place in the North-East part of the US power system in August 14th, 2003. The first signs of low voltage appeared 45 minutes prior to the cascading events and, during the events, the voltage levels dropped significantly in the entire system.

State estimation

The classic state estimation algorithms cannot use in the input measurement set voltage angle measurements, because of significant errors induced by the impossibility of accurate synchronization between measurements taken from buses around the system. The synchronization capabilities offered by the PMU devices coordinated via GPS overcomes this obstacle and the supplementary set of high precision measurements can contribute to a significant improving the estimation results, with minimal changes in the estimation mathematical models. Also, the technological advances and progressive development of PMU equipped monitoring systems made possible the new type of estimation algorithms used in wide area power system owned by several competitors: the distributed estimation (DE). DE algorithms divide the system into local subsystems, whose state is estimated independently, a minimal set of information being directed to a coordinator, which completes the global estimation. Voltage angle differences between subsystems can be compensated using PMU measurements installed in each subsystem [Jiang et.al. 07].

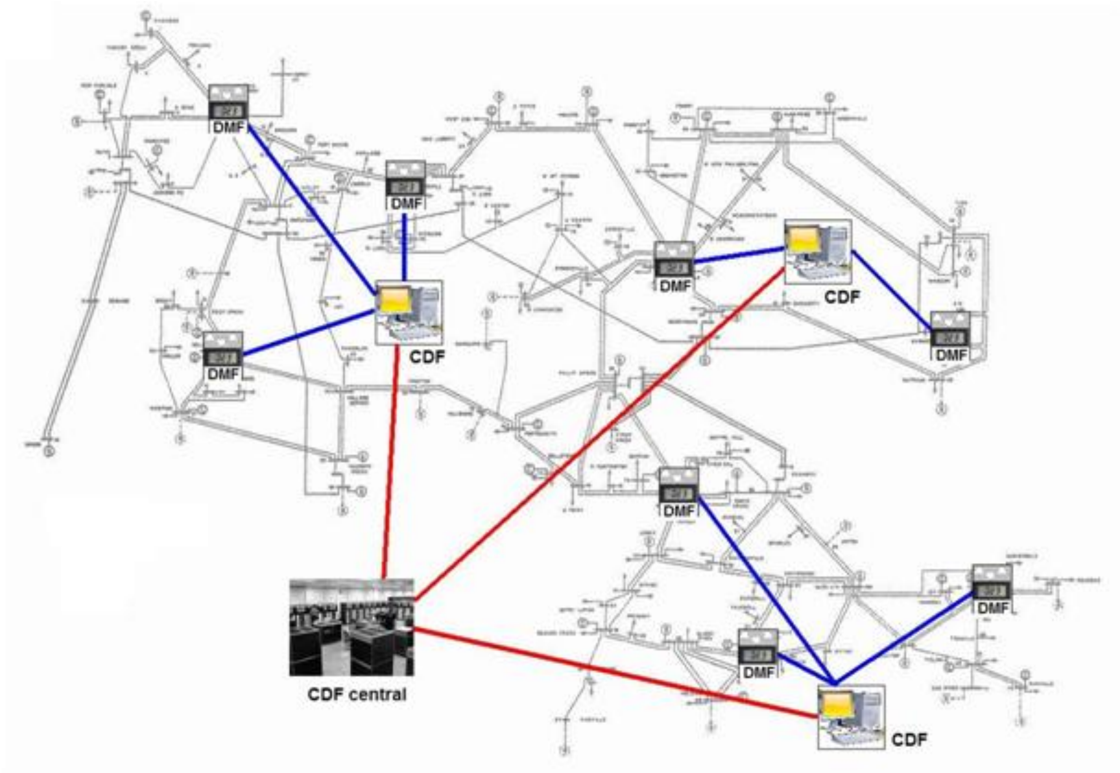

Fig. 12.2 – The multilayer PMU network architecture

(a) (b)

Fig. 12.3 – PMU equipments built by Macrodyne (a) and General Electric (b)

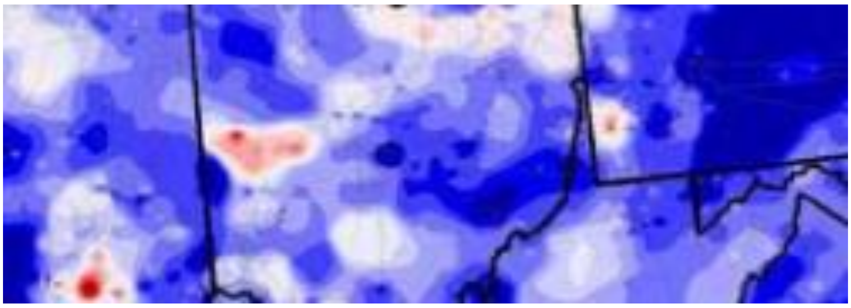

(a) The system in normal operation

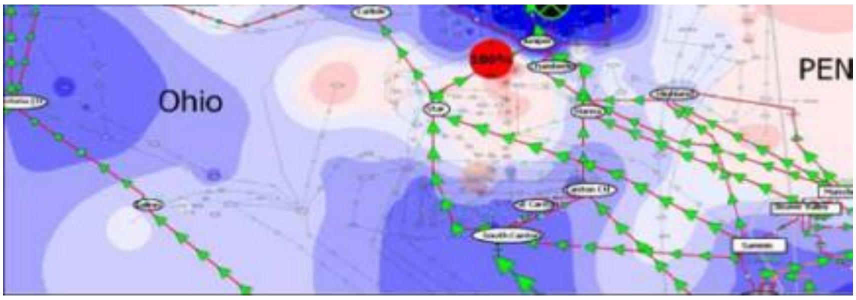

(b) The system with 45 minutes before the event

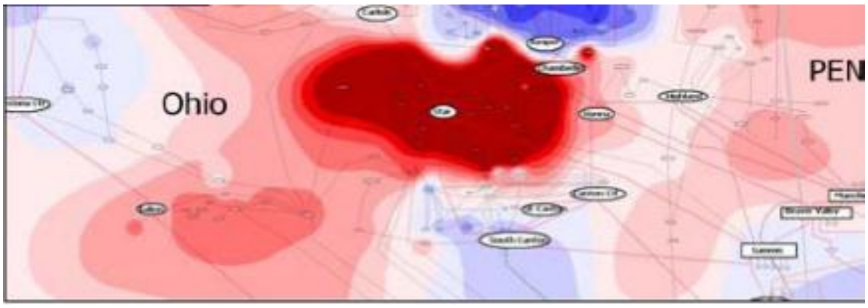

(c) Ther system during the cascading events

Voltage levels
in the system:

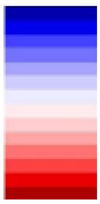

1.02 p.u.

0.95 p.u.

0.88 p.u.

Fig. 12.4. – Monitored voltage levels in the system during the August 14th 2003 US blackout

Congestion management

The standard method uses Nominal Transfer Capability, computed off-line using conservative hypothesis concerning thermal, voltage or stability limitations. The SPM technology uses synchronized measurements data from the congested branches, and computes the Real-time Transfer Capability for the actual operating conditions [Chakrabati et. al. 2009]. Another application is better controlling of transmission lines loading near to their real stability limits [Bertsch et. al. 2003].

New adaptive protection systems

New types of intelligent protection relays can be built using the SPM technology. The hardware level algorithms built in the relays can make decisions based on information received from nearby PMUs. Two promising applications in this field are line outage detection [Tate 2008] and high accuracy measurement of line impedance for fault-locating applications [Brahma 2007].

Post-mortem analysis

Classic methods use data taken previously in the system, which can be affected by lack of synchronization. Using PMU data, the time table of a contingency event can be reconstructed with higher precision.

12.4. Using phasor measurements in the WLS state estimation algorithm

The use of phasor measurements in the classic WLS algorithm has two main advantages:

- improved estimation precision, by adding accurate and, more important, synchronized angle measurements in the measurement set
- the mathematical model remains the same, the only changes occurring in the *H* Jacobian matrix, that must include lines and columns for the new bus voltage angle and branch current measurements

Updating the WLS mathematical model

For a *N* bus system, the state vector will contain 2**N*-1 unknown values, i.e. *N* bus voltage magnitudes and *N*-1 bus voltage angles. The known voltage angle is the one from the slack bus, which is set to 0. If the branches are represented through Π quadrupoles with lumped parameters (Fig. 12.5), any element from the bus admittance matrix $[Y_n]$ is written as $\underline{Y}_{ik}=G_{ik}+j*B_{ik}$, and the traditional measurement set will include

- Active and reactive bus powers,– P_i, Q_i
- Active and reactive branch power flows – P_{ik}, Q_{ik}
- Bus voltage magnitudes - U_i,

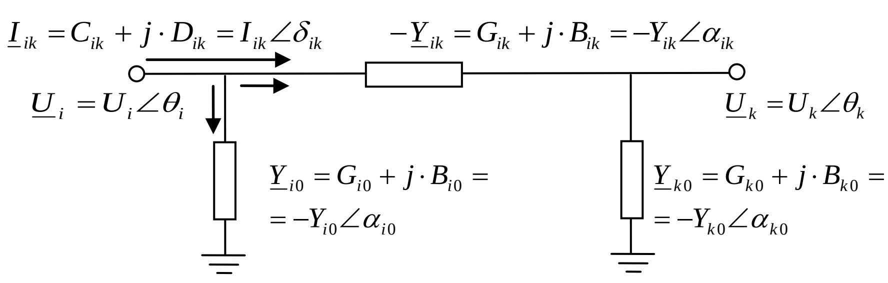

Fig. 12.5 - A Π quadrupole representation for branch elements

The bus and branch powers will be recomputed using the available approximation for voltages, as

$$\begin{aligned}
P_i &= G_{ii} \cdot U_i^2 + \sum_{\substack{k=1 \\ k\neq i}}^{N} U_i \cdot U_k \cdot (G_{ik} \cdot \cos\theta_{ik} + B_{ik} \cdot \sin\theta_{ik}) \\
Q_i &= -B_{ii} \cdot U_i^2 + \sum_{\substack{k=1 \\ k\neq i}}^{N} U_i \cdot U_k \cdot (G_{ik} \cdot \sin\theta_{ik} - B_{ik} \cdot \cos\theta_{ik}) \\
P_{ik} &= U_i^2 \cdot (g_{io} + g_{ik}) - U_i \cdot U_k (g_{ik} \cdot \cos\theta_{ik} + b_{ik} \cdot \sin\theta_{ik}) \\
Q_{ik} &= -U_i^2 \cdot (b_{io} + b_{ik}) - U_i \cdot U_k (g_{ik} \cdot \sin\theta_{ik} - b_{ik} \cdot \cos\theta_{ik})
\end{aligned} \tag{12.2}$$

The Jacobian elements for bus powers are computed as for the Newton-Raphson load flow method. To these are added Jacobian elements for

bus voltage magnitudes:

$$\begin{aligned}
&\frac{\partial U_i}{\partial \theta_i} = 0 \qquad && \frac{\partial U_i}{\partial U_i} = 1 \\
&\frac{\partial U_i}{\partial \theta_k} = 0 \qquad && \frac{\partial U_i}{\partial U_k} = 0
\end{aligned} \tag{12.3}$$

angles

$$\begin{aligned}
&\frac{\partial \theta_i}{\partial \theta_i} = 1 \qquad && \frac{\partial \theta_i}{\partial U_i} = 0 \\
&\frac{\partial \theta_i}{\partial \theta_k} = 0 \qquad && \frac{\partial \theta_i}{\partial U_k} = 0
\end{aligned} \tag{12.4}$$

and branch power flows:

$$\begin{aligned}
\frac{\partial P_{ik}}{\partial \theta_i} &= U_i \cdot U_k \cdot (g_{ik} \cdot \sin\theta_{ik} - b_{ik} \cdot \cos\theta_{ik}) \\
\frac{\partial P_{ik}}{\partial \theta_k} &= -U_i \cdot U_k \cdot (g_{ik} \cdot \sin\theta_{ik} - b_{ik} \cdot \cos\theta_{ik}) \\
\frac{\partial P_{ik}}{\partial U_i} &= -U_k \cdot (g_{ik} \cdot \cos\theta_{ik} + b_{ik} \cdot \sin\theta_{ik}) + 2 \cdot (g_{ik} + g_{i0}) \cdot U_i \\
\frac{\partial P_{ik}}{\partial U_k} &= -U_i \cdot (g_{ik} \cdot \cos\theta_{ik} + b_{ik} \cdot \sin\theta_{ik}) \\
\frac{\partial Q_{ik}}{\partial \theta_i} &= -U_i \cdot U_k \cdot (g_{ik} \cdot \cos\theta_{ik} + b_{ik} \cdot \sin\theta_{ik})
\end{aligned} \tag{12.5}$$

$$\frac{\partial Q_{ik}}{\partial \theta_k} = U_i \cdot U_k \cdot (g_{ik} \cdot \cos\theta_{ik} + b_{ik} \cdot \sin\theta_{ik})$$
$$\frac{\partial Q_{ik}}{\partial U_i} = -U_k \cdot (g_{ik} \cdot \sin\theta_{ik} - b_{ik} \cdot \cos\theta_{ik}) - 2 \cdot (b_{ik} + b_{i0}) \cdot U_i$$
$$\frac{\partial Q_{ik}}{\partial U_k} = -U_i \cdot (g_{ik} \cdot \sin\theta_{ik} - b_{ik} \cdot \cos\theta_{ik})$$

To include in the mathematical model derivatives for the currents measured on the branches connected in the PMU measured buses, the real and imaginary part of the current on any *i-k* branch are computed as [Gavrilaş 08]:

$$\begin{aligned}
C_{ik} &= I_{ik} \cdot \cos\delta_{ik} = \\
&= U_i \cdot Y_{i0} \cdot \cos(\theta_i + \alpha_{i0}) + U_k \cdot Y_{ik} \cdot \cos(\theta_k + \alpha_{ik}) - U_i \cdot Y_{ik} \cdot \cos(\theta_i + \alpha_{ik}) \\
D_{ik} &= I_{ik} \cdot \sin\delta_{ik} = \\
&= U_i \cdot Y_{i0} \cdot \sin(\theta_i + \alpha_{i0}) + U_k \cdot Y_{ik} \cdot \sin(\theta_k + \alpha_{ik}) - U_i \cdot Y_{ik} \cdot \sin(\theta_i + \alpha_{ik})
\end{aligned} \tag{12.6}$$

The corresponding Jacobian elements will result as:

$$\begin{aligned}
\frac{\partial C_{ik}}{\partial U_i} &= Y_{i0} \cdot \cos(\theta_i + \alpha_{i0}) - Y_{ik} \cdot \cos(\theta_i + \alpha_{ik}) \\
\frac{\partial C_{ik}}{\partial U_k} &= Y_{ik} \cdot \cos(\theta_k + \alpha_{ik}) \\
\frac{\partial C_{ik}}{\partial \theta_i} &= -U_i \cdot Y_{i0} \cdot \sin(\theta_i + \alpha_{i0}) + U_i \cdot Y_{ik} \cdot \sin(\theta_i + \alpha_{ik}) \\
\frac{\partial C_{ik}}{\partial \theta_k} &= -U_k \cdot Y_{ik} \cdot \sin(\theta_k + \alpha_{ik})
\end{aligned} \tag{12.7}$$

and

$$\begin{aligned}
\frac{\partial D_{ik}}{\partial U_i} &= Y_{i0} \cdot \sin(\theta_i + \alpha_{i0}) - Y_{ik} \cdot \sin(\theta_i + \alpha_{ik}) \\
\frac{\partial D_{ik}}{\partial U_k} &= Y_{ik} \cdot \sin(\theta_k + \alpha_{ik}) \\
\frac{\partial D_{ik}}{\partial \theta_i} &= U_i \cdot Y_{i0} \cdot \cos(\theta_i + \alpha_{i0}) - U_i \cdot Y_{ik} \cdot \cos(\theta_i + \alpha_{ik}) \\
\frac{\partial D_{ik}}{\partial \theta_k} &= U_k \cdot Y_{ik} \cdot \cos(\theta_k + \alpha_{ik})
\end{aligned} \tag{12.8}$$

The algorithm will use the updated measurement set and Jacobian matrix and compute the state vector in the same manner as the classic WLS algorithm.

2.5. Example 1
Acquiring and using data from a PMU installed in the system

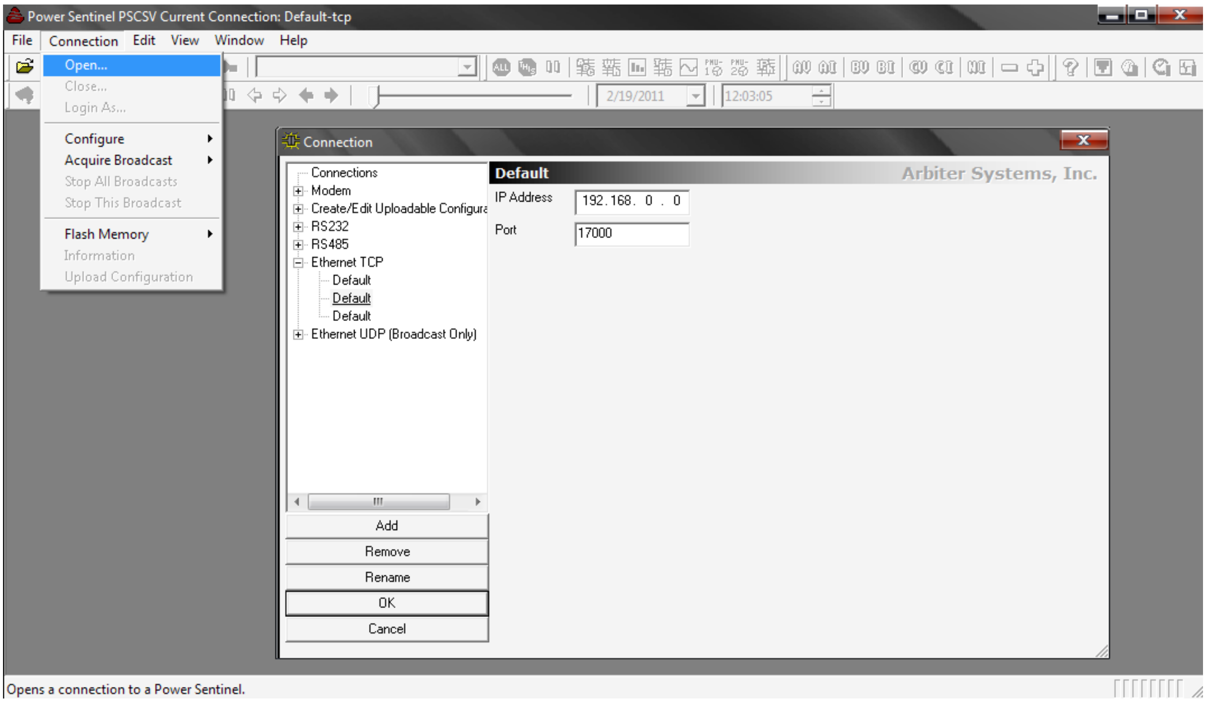

Fig. 12.6 – Connecting to a PMU in the system via a Ethernet communications network

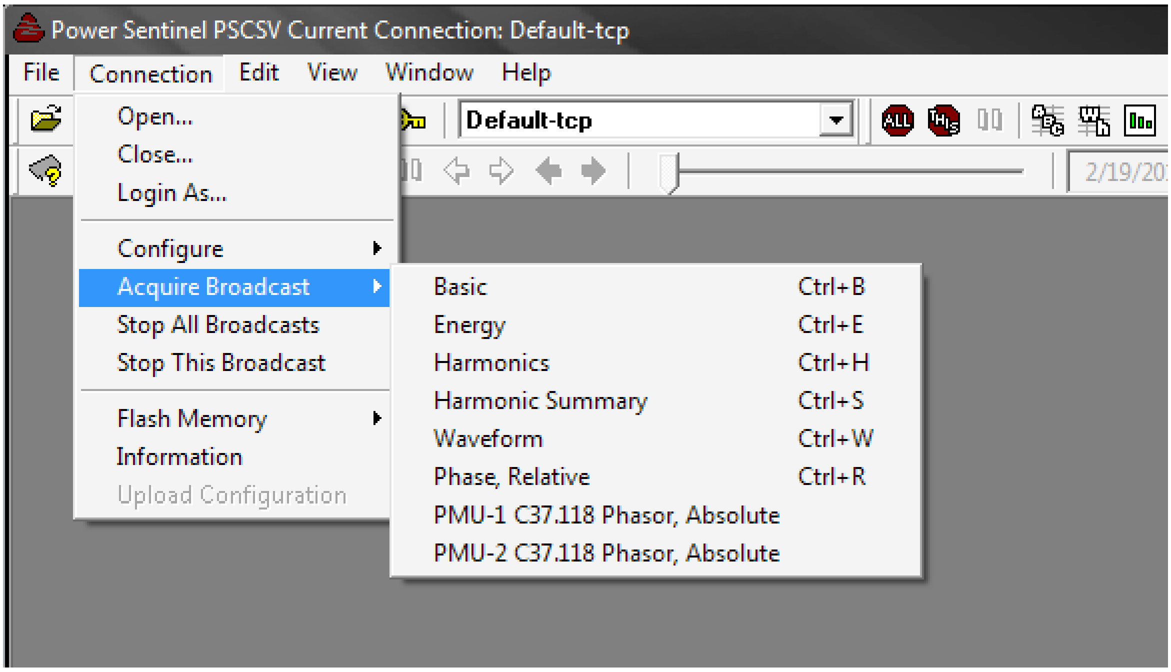

Fig. 12.7 – Choosing what data to view and/or save

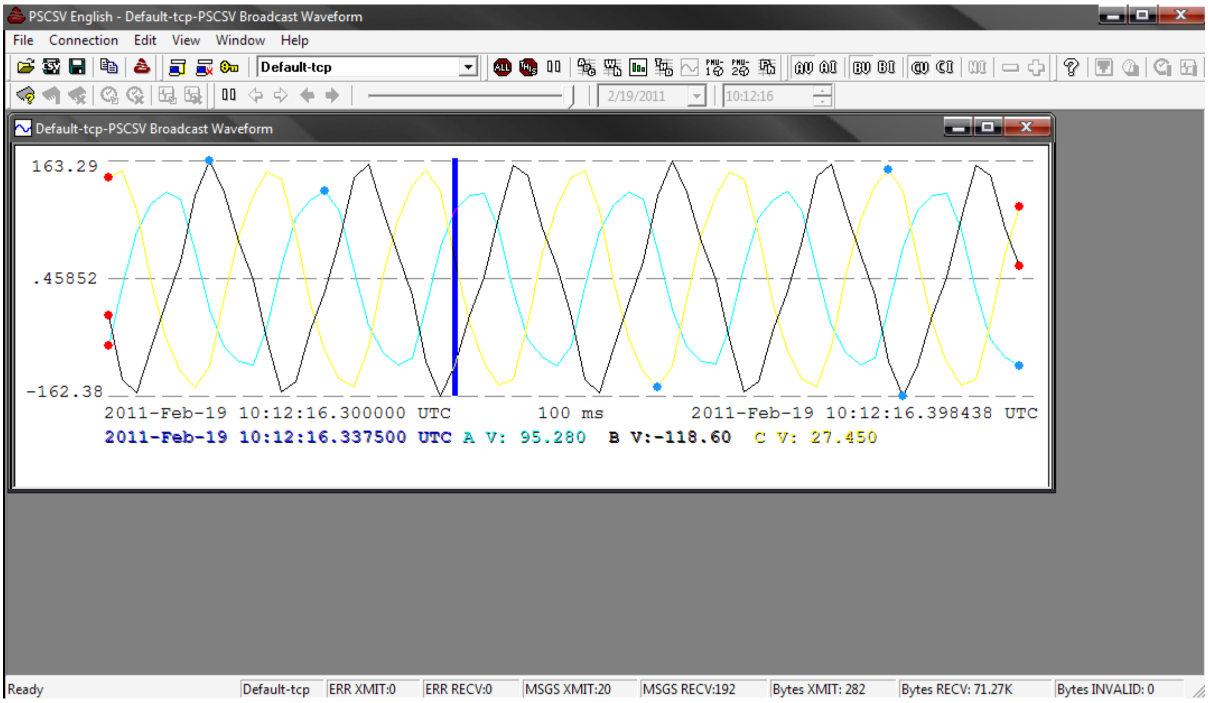

Fig. 12.8 – Acquiring data (A-B-C phase voltage waveform)

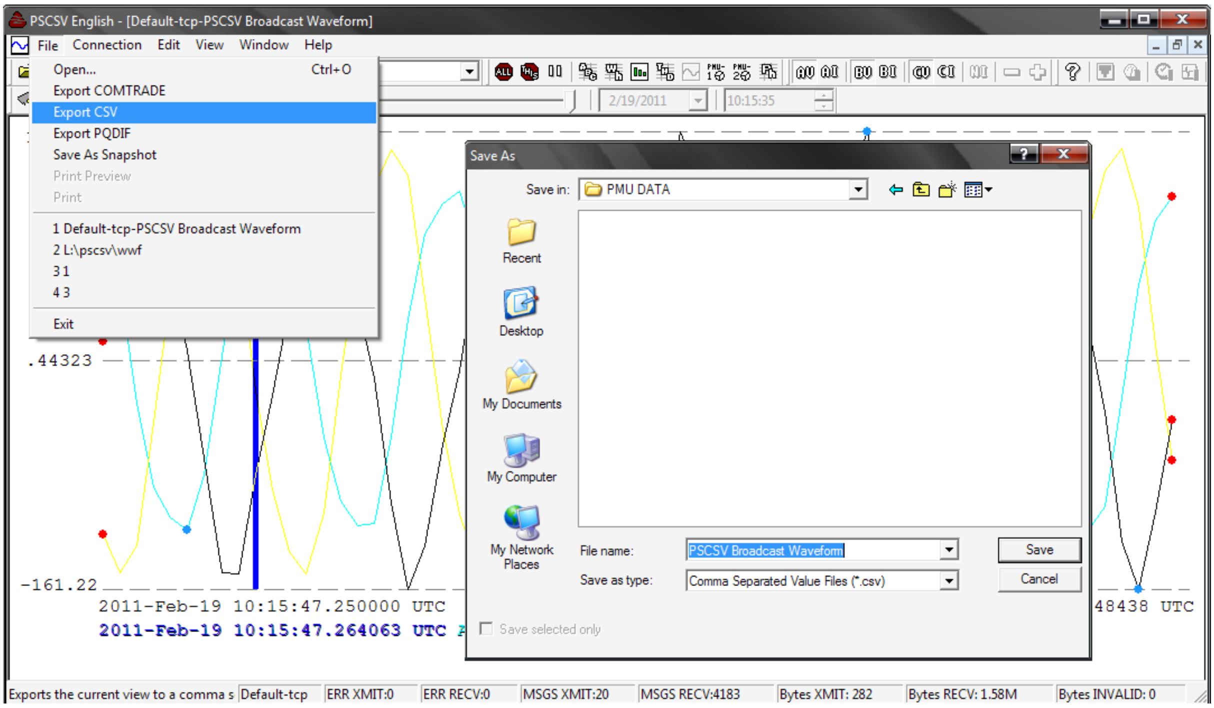

Fig. 12.9 – Saving data in CSV format for later use

Table 12.1 – Sample data for the recoded waveforms (A-B-C voltages and currents)

UTC Time	A V	A I	B V	B I	C V	C I
2011-Feb-19 10:12:07.600000 UTC	-67.219	-0.88242	-82.717	-0.2201	145.9622	0.71633
2011-Feb-19 10:12:07.601563 UTC	16.84297	-0.20277	-155.347	-0.87936	137.8922	0.69493
2011-Feb-19 10:12:07.603125 UTC	83.54234	0.45751	-141.408	-1.16773	61.41111	0.33524
2011-Feb-19 10:12:07.604688 UTC	109.5863	0.78256	-70.8566	-0.88548	-34.3279	-0.26289
2011-Feb-19 10:12:07.606250 UTC	120.927	0.92929	-16.5984	-0.57775	-98.8569	-0.71939
2011-Feb-19 10:12:07.607813 UTC	92.80445	0.81109	51.69049	-0.22417	-137.953	-0.94661
2011-Feb-19 10:12:07.609375 UTC	11.58527	0.20991	139.4818	0.4351	-146.757	-0.99654
2011-Feb-19 10:12:07.610938 UTC	-65.2321	-0.49827	157.792	0.90687	-92.7739	-0.7683
2011-Feb-19 10:12:07.612500 UTC	-102.556	-0.93744	94.36342	0.76422	5.89962	-0.19564
2011-Feb-19 10:12:07.614063 UTC	-118.42	-1.12493	34.57241	0.42898	80.88293	0.32607

Example 2 – Measurement set and Jacobian matrix for the WLS algorithm with phasor measurements

For a simple 5 bus system (Fig. 12.10), the following measurement set is available:

N1 – bus voltage magnitude, U_1

N4 and N5: active and reactive bus powers $P_4, P_5, Q_4, Q_5,$

$P_{3\text{-}4}$, $Q_{3\text{-}4}$ – branch power flow measured in the end connected to bus N4

At bus N2, a PMU is installed, which will provide bus voltage magnitude and angle measurements in bus N2 and branch current measurements for branches.B1-2 and B2-3.

The state vector *[x]*, measurement vector *[z]* and Jacobian matrix *[H]* are presented below. The values marked with bold font face denote values added by phasor measurements

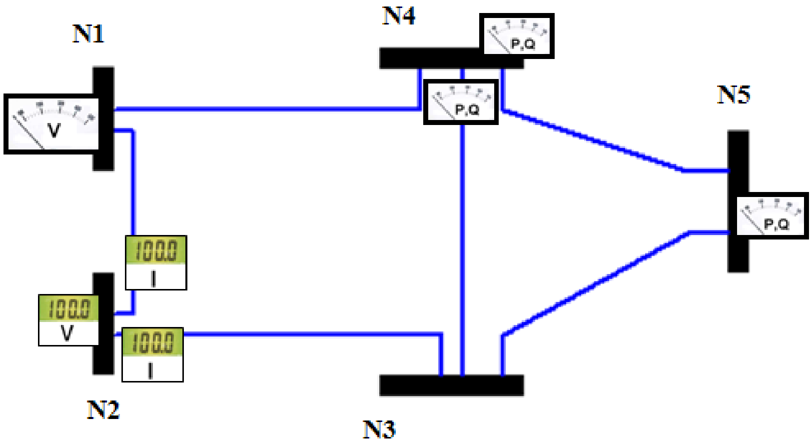

Fig. 12.10 – An example of including phasor measurements in the WLS algorithm

$[H] =$

$\partial P_4/\partial U_1$	$\partial P_4/\partial U_2$	$\partial P_4/\partial U_3$	$\partial P_4/\partial U_4$	$\partial P_4/\partial U_5$	$\partial P_4/\partial \theta_1$	$\partial P_4/\partial \theta_2$	$\partial P_4/\partial \theta_3$	$\partial P_4/\partial \theta_4$	$\partial P_4/\partial \theta_5$
$\partial P_5/\partial U_1$	$\partial P_5/\partial U_2$	$\partial P_5/\partial U_3$	$\partial P_5/\partial U_4$	$\partial P_5/\partial U_5$	$\partial P_5/\partial \theta_1$	$\partial P_5/\partial \theta_2$	$\partial P_5/\partial \theta_3$	$\partial P_5/\partial \theta_4$	$\partial P_5/\partial \theta_5$
$\partial Q_4/\partial U_1$	$\partial Q_4/\partial U_2$	$\partial Q_4/\partial U_3$	$\partial Q_4/\partial U_4$	$\partial Q_4/\partial U_5$	$\partial Q_4/\partial \theta_1$	$\partial Q_4/\partial \theta_2$	$\partial Q_4/\partial \theta_3$	$\partial Q_4/\partial \theta_4$	$\partial Q_4/\partial \theta_5$
$\partial Q_5/\partial U_1$	$\partial Q_5/\partial U_2$	$\partial Q_5/\partial U_3$	$\partial Q_5/\partial U_4$	$\partial Q_5/\partial U_5$	$\partial Q_5/\partial \theta_1$	$\partial Q_5/\partial \theta_2$	$\partial Q_5/\partial \theta_3$	$\partial Q_5/\partial \theta_4$	$\partial Q_5/\partial \theta_5$
$\partial P_{43}/\partial U_1$	$\partial P_{43}/\partial U_2$	$\partial P_{43}/\partial U_3$	$\partial P_{43}/\partial U_4$	$\partial P_{43}/\partial U_5$	$\partial P_{43}/\partial \theta_1$	$\partial P_{43}/\partial \theta_2$	$\partial P_{43}/\partial \theta_3$	$\partial P_{43}/\partial \theta_4$	$\partial P_{43}/\partial \theta_5$
$\partial Q_{43}/\partial U_1$	$\partial Q_{43}/\partial U_2$	$\partial Q_{43}/\partial U_3$	$\partial Q_{43}/\partial U_4$	$\partial Q_{43}/\partial U_5$	$\partial Q_{43}/\partial \theta_1$	$\partial Q_{43}/\partial \theta_2$	$\partial Q_{43}/\partial \theta_3$	$\partial Q_{43}/\partial \theta_4$	$\partial Q_{43}/\partial \theta_5$
$\partial U_1/\partial U_1$	$\partial U_1/\partial U_2$	$\partial U_1/\partial U_3$	$\partial U_1/\partial U_4$	$\partial U_1/\partial U_5$	$\partial U_1/\partial \theta_1$	$\partial U_1/\partial \theta_2$	$\partial U_1/\partial \theta_3$	$\partial U_1/\partial \theta_4$	$\partial U_1/\partial \theta_5$
$\boldsymbol{\partial U_2/\partial U_1}$	$\boldsymbol{\partial U_2/\partial U_2}$	$\boldsymbol{\partial U_2/\partial U_3}$	$\boldsymbol{\partial U_2/\partial U_4}$	$\boldsymbol{\partial U_2/\partial U_5}$	$\boldsymbol{\partial U_2/\partial \theta_1}$	$\boldsymbol{\partial U_2/\partial \theta_2}$	$\boldsymbol{\partial U_2/\partial \theta_3}$	$\boldsymbol{\partial U_2/\partial \theta_4}$	$\boldsymbol{\partial U_2/\partial \theta_5}$
$\boldsymbol{\partial \theta_2/\partial U_1}$	$\boldsymbol{\partial \theta_2/\partial U_2}$	$\boldsymbol{\partial \theta_2/\partial U_3}$	$\boldsymbol{\partial \theta_2/\partial U_4}$	$\boldsymbol{\partial \theta_2/\partial U_5}$	$\boldsymbol{\partial \theta_2/\partial \theta_1}$	$\boldsymbol{\partial \theta_2/\partial \theta_2}$	$\boldsymbol{\partial \theta_2/\partial \theta_3}$	$\boldsymbol{\partial \theta_2/\partial \theta_4}$	$\boldsymbol{\partial \theta_2/\partial \theta_5}$
$\boldsymbol{\partial C_{23}/\partial U_1}$	$\boldsymbol{\partial C_{23}/\partial U_2}$	$\boldsymbol{\partial C_{23}/\partial U_3}$	$\boldsymbol{\partial C_{23}/\partial U_4}$	$\boldsymbol{\partial C_{23}/\partial U_5}$	$\boldsymbol{\partial C_{23}/\partial \theta_1}$	$\boldsymbol{\partial C_{23}/\partial \theta_2}$	$\boldsymbol{\partial C_{23}/\partial \theta_3}$	$\boldsymbol{\partial C_{23}/\partial \theta_4}$	$\boldsymbol{\partial C_{23}/\partial \theta_5}$
$\boldsymbol{\partial C_{21}/\partial U_1}$	$\boldsymbol{\partial C_{21}/\partial U_2}$	$\boldsymbol{\partial C_{21}/\partial U_3}$	$\boldsymbol{\partial C_{21}/\partial U_4}$	$\boldsymbol{\partial C_{21}/\partial U_5}$	$\boldsymbol{\partial C_{21}/\partial \theta_1}$	$\boldsymbol{\partial C_{21}/\partial \theta_2}$	$\boldsymbol{\partial C_{21}/\partial \theta_3}$	$\boldsymbol{\partial C_{21}/\partial \theta_4}$	$\boldsymbol{\partial C_{21}/\partial \theta_5}$
$\boldsymbol{\partial D_{23}/\partial U_1}$	$\boldsymbol{\partial D_{23}/\partial U_2}$	$\boldsymbol{\partial D_{23}/\partial U_3}$	$\boldsymbol{\partial D_{23}/\partial U_4}$	$\boldsymbol{\partial D_{23}/\partial U_5}$	$\boldsymbol{\partial D_{23}/\partial \theta_1}$	$\boldsymbol{\partial D_{23}/\partial \theta_2}$	$\boldsymbol{\partial D_{23}/\partial \theta_3}$	$\boldsymbol{\partial D_{23}/\partial \theta_4}$	$\boldsymbol{\partial D_{23}/\partial \theta_5}$
$\boldsymbol{\partial D_{21}/\partial U_1}$	$\boldsymbol{\partial D_{21}/\partial U_2}$	$\boldsymbol{\partial D_{21}/\partial U_3}$	$\boldsymbol{\partial D_{21}/\partial U_4}$	$\boldsymbol{\partial D_{21}/\partial U_5}$	$\boldsymbol{\partial D_{21}/\partial \theta_1}$	$\boldsymbol{\partial D_{21}/\partial \theta_2}$	$\boldsymbol{\partial D_{21}/\partial \theta_3}$	$\boldsymbol{\partial D_{21}/\partial \theta_4}$	$\boldsymbol{\partial D_{21}/\partial \theta_5}$

$[z] = [P_4 \quad P_5 \quad Q_4 \quad Q_5 \quad P_{43} \quad Q_{43} \quad U_1 \quad \boldsymbol{U_2} \quad \boldsymbol{\Theta_2} \quad \boldsymbol{C_{23}} \quad \boldsymbol{C_{21}} \quad \boldsymbol{D_{23}} \quad \boldsymbol{D_{21}}]^T$

$[x] = [U_1 \quad U_2 \quad U_3 \quad U_4 \quad U_5 \quad \Theta_1 \quad \Theta_2 \quad \Theta_3 \quad \Theta_4 \quad \Theta_5]$

References:

[Bertsch et.al. 2003] Bertsch, J. Zima, M. Suranyi, A. Carnal, C. Rehtanz, C. - Experiences with and perspectives of the system for wide area monitoring of power systems, CIGRE/IEEE PES International Symposium on Quality and Security of Electric Power Delivery Systems, 8-10 Oct. 2003, pp. 5-9.

[Brahma 2007] Brahma S.M. - Iterative Fault Location Scheme for a Transmission Line Using Synchronized Phasor Measurements, International Journal of Emerging Electric Power Systems, Vol.8, No. 6, 2007, pp.1-14.

[Bonanomi 1981] Bonanomi P. - Phase Angle Measurements with Synchronized Clocks - Principle and Applications, Trans. of IEEE on PAS, Vol. PAS-100, No. 12, Dec 1981, p 5036.

[Bukh 07] Bukh B., Gudmundsdottir U. S., Holst P. B, Jensen K. B., Jensen L.C., Bak C.L - Advantages in using Kalman phasor estimation in numerical differential protective relaying compared to the Fourier estimation method, International Conference on Power Systems Transients (IPST'07) in Lyon, France, June 4-7, 2007

[Chakrabarti et. al. 09] Chakrabarti S., Kyriakides, E., Tianshu Bi, Deyu Cai, Measurements get together, IEEE Power and Energy Magazine, Vol. 7, No. 1, 2009, pp. 41-49.

[Gavrilas 08] Gavrilas M. - Aspecte moderne în modelarea sistemelor electroenergetice, Editura Venus, Iasi, 2008

[Gavrilaş 09] Gavrilaş M - Recent Advances and Applications of Synchronized Phasor Measurements in Power Systems, Proc. Of the 9th WSEAS/IASME International Conference On Electric Power Systems, High Voltages, Electric machines (POWER '09). Vol. Recent Advances in Electric Power Systems, High Voltages, Electric Machines, ISSN 1790-5117, pp. 82 – 91

[Jiang et. al 07] Jiang W., Vittal V., Heydt G. – A Distributed State Estimator Utilizing Sznchrronized Phasor Measurements, IEEE Trans. On Power Systems, Vol. 22, No.2, pp. 563 – 571, May 2007

[Jordan 08] Jordan J., van Wyk A., van Wyk B. - Nonparametric Time-Varying Phasor Estimation Using Neural Networks, Lecture Notes in Computer Science, Volume 4985/2008, June 29, 2008, ISSN 0302-9743, pp. 693-702.

[Karlsson 2004] Karlsson D., Hemmingsson M., Lindahl S. - Wide Area Monitoring and Control – Terminology, Phenomena and Solutions Implementation Strategies, IEEE Power & Energy Magazine, Vol. 2, No. 5, 2004, pp. 68-76.

[Martin 2008] Martin K.E. and Carroll J.R. - Phasing in the Technology, IEEE Power and Energy Magazine, Vol. 6, Issue 5, Sept-Oct. 2008, pp. 24-33.

[Pajic 07] Pajic S. - Power System State Estimation and Contingency Constrained Optimal Power Flow - A Numerically Robust Implementation, PH.D Dissertation for the Worcester Polytechnic Institute, pp., April 2007

[Phadke et al 1983] Phadke A.G., Thorp J.S., Adamiak M.G. - A New Measurement Technique for Tracking Voltage Phasors, Local Frequency, and Rate of Change of Frequency, Trans. of IEEE on PAS, Vol. PAS-102 No. 5, May 1983, pp 1025-1038.

[Phadke 2002] Phadke A.G. - Synchronized Phasor Measurements – A Historical Overview, 2002 IEEE/PES Transmission and Distribution Conference and Exposition, Asia Pacific, Vol. 1, Oct. 2002, pp. 476-479.

[Tate 2008] Tate J.E., Overbye T.J. - Line Outage Detection Using Phasor Angle Measurements, IEEE Trans. on Power Systems, Vol. 23, No. 4, Nov. 2008, pp. 1644-1652.

[webMicro] http://www.macrodyneusa.com/model_1690.htm

[webGE] http://www.gedigitalenergy.com/multilin/newproducts.htm